PAPER 24

HARMONIC ANALYSIS OF THE PERIODIC SPECTRUM VARIABLES

ARMIN J. DEUTSCH

Mount Wilson and Palomar Observatories, Pasadena, California, U.S.A.

ABSTRACT

Certain stars are known to be periodic magnetic variables, and to show synchronous changes in line strength and radial velocity. The hypothesis has been made that the atmosphere of such a star is in rigid rotation, and that it is characterized by a permanent magnetic field and associated abundance irregularities. The magnetic potential and the local equivalent widths have been developed in spherical harmonics, and the Laplace coefficients of these expansions have been related to the Fourier coefficients of the observed curves. The theory has been applied to the star HD 125248 in an attempt to verify the original hypothesis and to map the magnetic fields and abundance anomalies over the stellar atmospheres.

Among the stars in which H. W. Babcock has found spectroscopic evidence of a general magnetic field [1], there are several that show periodic reversals of the observed field. In addition, some of these stars exhibit synchronous variations in the equivalent widths of certain absorption lines, and in the radial velocities indicated by these lines. These phenomena are illustrated for the star HD 125248 ($P = 9{\cdot}30$ days) in Figs. 1, 2 and 3.

Fig. 1 is taken from the work of Babcock [2]. He has converted the effective field H_e, as found from the observed Zeeman effect, into the polar field H_p, on the assumption that the field is that of a dipole viewed along the axis. The figure shows that different elements sometimes indicate significantly different values for H_p. Fig. 2 is based on 13 coudé spectrograms at 4·5 Å/mm, obtained by Babcock and Deutsch during one cycle in 1951 and one cycle in 1952. The figure rests on spectrophotometric measures of 127 different absorption lines chosen to be relatively free from blends. When the measured equivalent widths W of each line are expressed in units of its average equivalent width $\overline{W}$ at all observed phases, it is found that, within the errors of observation, all lines of a given element show nearly the same variation with phase. Moreover, among the nine elements discussed, each can be

assigned to one of three groups, within each of which the intensity variation is the same. Fig. 2 shows how this assignment has been made. The mean points have been obtained by weighting each element in the group with the number of its lines that were measured.

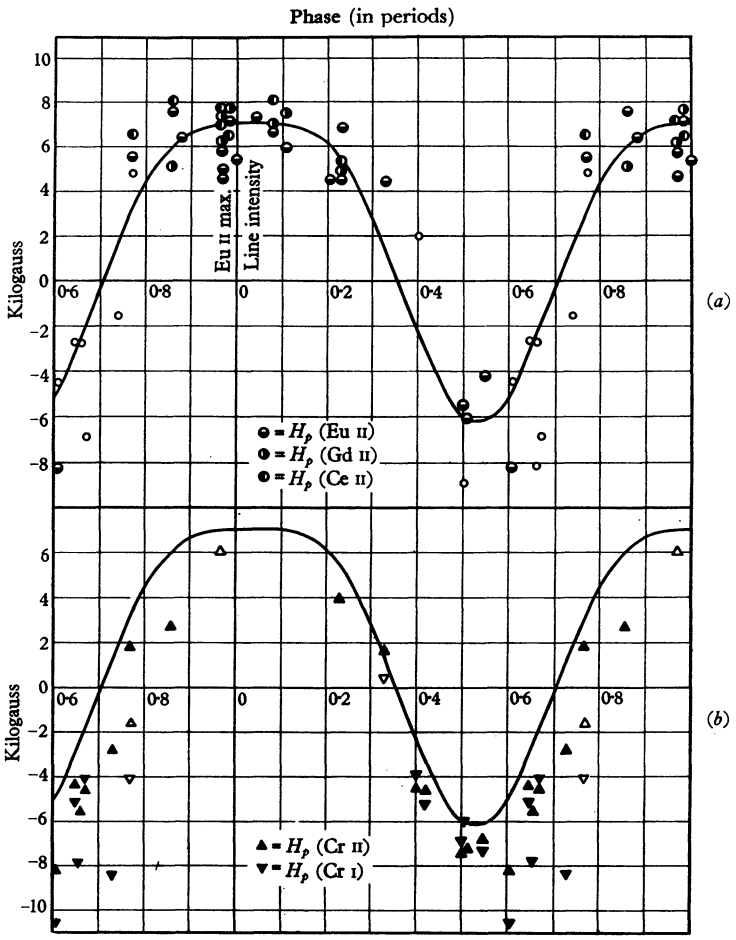

Fig. 1 (*a*). Magnetic field intensity, H_p, in kilogauss, for the rare earths, plotted against phase. Small open circles are of low weight. For comparison, the smooth curve for the Fe–Ti lines is also shown. Fig. 1 (*b*). Similar results for Cr I and Cr II. (Reproduced from the *Astrophysical Journal*.)

Fig. 3 is based on radial-velocity measures of the eight 1951 coudé spectrograms. As far as possible, all lines measured for intensity were also measured for velocity, and no others. With the possible exception of Sr II, for which only two lines could be measured, the same group behavior prevails in the radial velocities as in the equivalent widths. The details of

the observations summarized in these figures will be discussed later in another publication. This is also true of the mathematical developments to be outlined below.

It has been proposed that the atmosphere of such a star as HD 125248 is

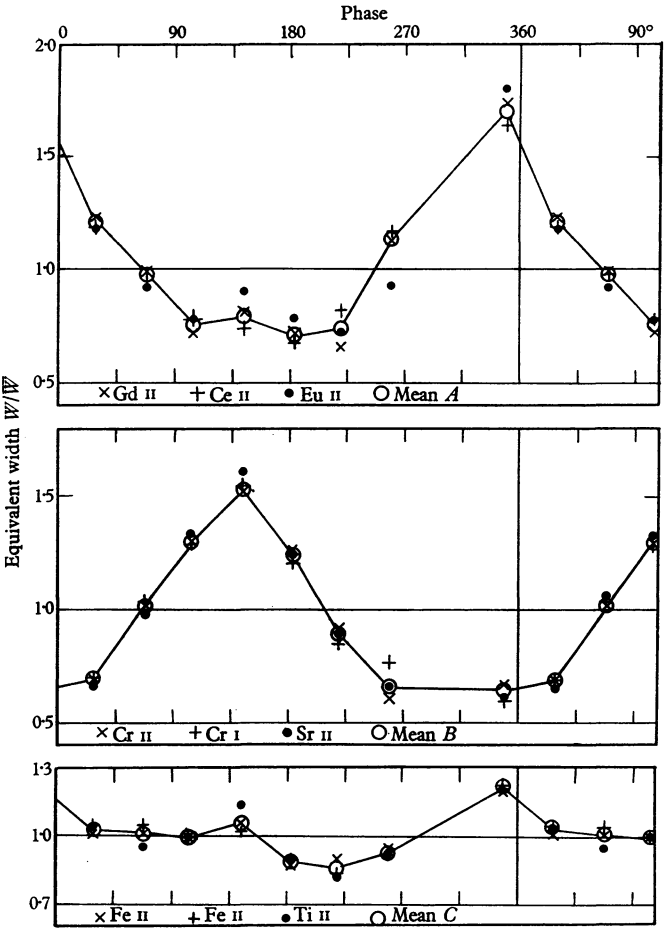

Fig. 2. Equivalent widths of 127 absorption lines. For each line, the measured equivalent width W has been divided by the average measured equivalent width $\overline{W}$ at all observed phases. For a given element at a given phase, the plotted point is the average value of $W/\overline{W}$ for all lines of that element.

spectroscopically non-homogeneous, and that it is in rigid rotation around an axis that is not a symmetry axis of the abundance irregularities or of the associated general magnetic field. The observed variations would then be attributed to the changing aspect of the star as it rotates; the observed period would be simply the period of rotation. The observations cannot all

be satisfied with such a model if the abundance irregularities and/or magnetic field possess symmetry axes. It appears, however, that a satisfactory representation may be possible by a more general kind of rigid rotator. The evidence for this type of model has recently been summarized elsewhere [3].

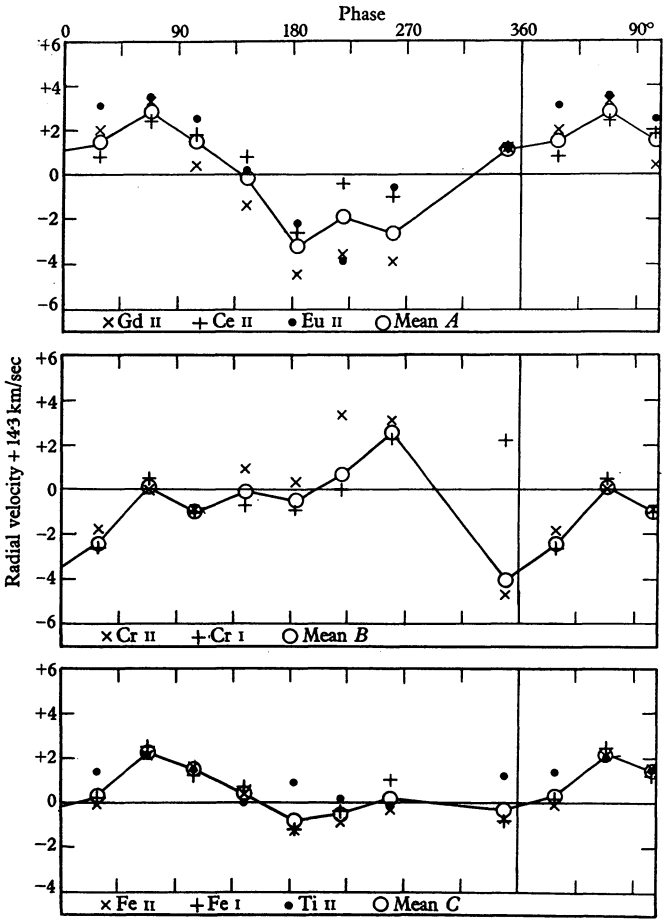

Fig. 3. Radial velocities from 127 absorption lines.
The systemic velocity is $V_0 = -14{\cdot}3$ km/sec.

Fig. 4 represents a spherical star with the pole of rotation at P_0 and the subpolar point at S, the inclination of the rotational axis to the line of sight being χ. At an arbitrary point P on the surface, the polar distance is ψ and the azimuth v. The latter angle is measured from a meridian that rotates with the star, with $v = 0$ along the meridian that passes through S at the

https://doi.org/10.1017/S0074180900237807 Published online by Cambridge University Press

phase $\Phi = 0$. The angle between S and P is θ, and the azimuthal angle around S is ϕ, with $\phi = \pi$ at P_0.

We shall call $\xi(\psi, v)$ the distribution function for a given spectrum line. Its value is the local equivalent width of the line at P in light emergent normally, and its variation reflects the abundance irregularities over the surface of the star. In general, we may represent $\xi(\psi, v)$ as the real part of a Laplace series,

$$\Xi(\psi, v) = \langle W \rangle \sum_{n=0}^{\infty} \sum_{m=-n}^{n} A_n^m \exp(imv)\, P_n^{|m|}(\cos \psi), \tag{1}$$

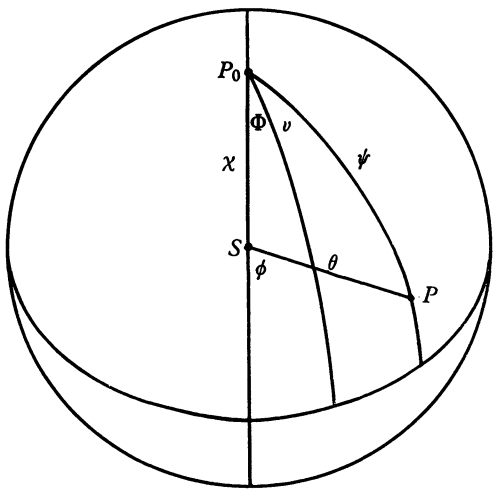

Fig. 4. Geometry of an oblique rotator. See text.

where $\langle W \rangle$ is the observed equivalent width averaged over the cycle of variation. To the extent that we can approximate the curve of growth by a straight line, it can be shown that all lines originating in a given group of elements will be characterized by the same set of Laplace coefficients A_n^m. Our first object will now be to compute the observed equivalent width W, in the integrated light from the visible hemisphere, as a function of the coefficients A_n^m and the phase Φ. We shall then compute the integrated radial velocity and Zeeman effect. Finally, we shall invert the argument and find the A_n^m from the observations of HD 125248.

We shall suppose that in the continuum the intensity is distributed over the stellar disk in the usual way, with the limb-darkening law

$$\Lambda = 1 - \mu + \mu \cos \theta. \tag{2}$$

We shall also take account, in an approximate way, of the variation of equivalent width with angle of emergence at a given point. We suppose

that the local equivalent width in the direction θ can be written in the form $\xi(\psi, v)\, J(\theta)$, where

$$J = 1 - \kappa + \kappa \cos\theta. \tag{3}$$

The quantity κ is then a coefficient of line-weakening toward the limb, analogous to the coefficient μ of limb-darkening in the continuum.

In order to find the observed equivalent width W in the integrated light from the visible hemisphere, we must weight the local equivalent width ξJ with the local surface brightness Λ and the projected element of area at P, and then integrate over the visible hemisphere. Similarly, the observed radial velocity V (relative to the systemic radial velocity V_0) will be obtained by inserting the local radial velocity of rotation as an additional weighting factor, and integrating over the visible hemisphere. If V_e is the equatorial speed of rotation, the line-of-sight component of the local rotational velocity is $V_e \sin x \sin\theta \sin\phi$ at P. Again, to find the effective magnetic field, we must insert the line-of-sight component H_z of the local magnetic field **H** as the additional weighting factor. We then find that the observed quantities W, V and H_e can be taken as the real parts of the following expressions:

$$\mathscr{W} = \frac{\int_0^{\pi/2}\int_0^{2\pi} (\Xi J)\, \Lambda \sin\theta \cos\theta \, d\phi \, d\theta}{\int_0^{\pi/2}\int_0^{2\pi} \Lambda \sin\theta \cos\theta \, d\phi \, d\theta}, \tag{4}$$

$$\mathscr{V} = \frac{\int_0^{\pi/2}\int_0^{2\pi} (V_e \sin\chi \sin\theta \sin\phi)\, (\Xi J)\, \Lambda \sin\theta \cos\theta \, d\phi \, d\theta}{\int_0^{\pi/2}\int_0^{2\pi} (\xi J)\, \Lambda \sin\theta \cos\theta \, d\phi \, d\theta}, \tag{5}$$

$$\mathscr{H}_e = \frac{\frac{1}{2}\int_0^{\pi/2}\int_0^{2\pi} H_z[(\Xi + \tilde{\Xi})\, J]\, \Lambda \sin\theta \cos\theta \, d\phi \, d\theta}{\int_0^{\pi/2}\int_0^{2\pi} (\xi J)\, \Lambda \sin\theta \cos\theta \, d\phi \, d\theta}. \tag{6}$$

To evaluate these integrals, it is necessary to express the distribution function Ξ in the alternative Laplace series

$$\Xi(\psi, v) = \langle W \rangle \sum_{n=0}^{\infty} \sum_{m=-n}^{n} B_n^m \exp(im\phi)\, P_n^{|m|}(\cos\theta), \tag{7}$$

in which the coefficients B_n^m are functions of χ and Φ, and of the coefficients A_n^m. This transformation has recently been fully discussed by Satô [4].

With his results, it is possible to show that the integrals of interest can be put in the form of Fourier series in the phase, as follows:

$$\frac{\mathscr{W}}{\langle W\rangle} = \sum_{m=0}^{\infty} D_{-m} \exp(-im\Phi), \tag{8}$$

$$\left(\frac{W}{\langle W\rangle}\right)\mathscr{V} = (V_e \sin\chi) \sum_{m=0}^{\infty} E_{-m} \exp(-im\Phi), \tag{9}$$

$$\left(\frac{W}{\langle W\rangle}\right)\mathscr{H}_e = \sum_{m=-\infty}^{\infty} G_m \exp(im\Phi). \tag{10}$$

The Fourier coefficients in these expressions are related to the Laplace coefficients by the equations

$$D_{-m} = \sum_{n=0}^{\infty} \mathscr{P}_n^m A_n^m, \tag{11}$$

$$E_{-m} = \sum_{n=0}^{\infty} \mathscr{Q}_n^m A_n^m, \tag{12}$$

$$G_m = \sum_{n=1}^{\infty}\sum_{\alpha=0}^{\infty}\sum_{\beta=0}^{\infty} M_n^\beta (F_1 A_\alpha^{-m-\beta} + F_2 \tilde{A}_\alpha^{m+\beta}). \tag{13}$$

In these equations, the quantities $\mathscr{P}_n^m$, $\mathscr{Q}_n^m$, $F_1(n, \alpha, m, \beta)$, and $F_2(n, \alpha, m, \beta)$ depend only on the indicated indices, and upon the limb-coefficients μ and κ. They have been obtained explicitly by a term-by-term integration of Eqs. (4), (5) and (6), after substitution of Eq. (7) into these integrals. The coefficients M_n^β characterize the complex magnetic field $\mathscr{H}$, which we suppose can be obtained from a scalar potential,

$$\mathscr{S} = R \sum_{n=1}^{\infty}\sum_{\beta=0}^{n} (R/r)^{n+1} M_n^\beta \exp(i\beta\upsilon)\, P_n^\beta(\cos\psi), \tag{14}$$

where R is the stellar radius. In obtaining Eqs. (11), (12) and (13), it has been assumed that $A_n^m \equiv 0$ for $m < 0$. This assumption entails no loss of generality for the real distribution function $\xi(\psi, \upsilon)$.

The observed curves corresponding to Eqs. (8), (9) and (10) can be reasonably well represented by Fourier series of the second degree. Accordingly, we shall suppose that we can obtain an adequate representation of the large-scale structure of the field and the abundance irregularities by considering only terms to the second degree in the Laplace expansions for Ξ and $\mathscr{S}$. When this is done, we find that the total number of real Laplace coefficients required to specify the magnetic potential, and the distribution functions for elements of groups A, B and C, is 35. Additional free parameters that must be specified to determine the observed curves are the

inclination χ of the rotational axis to the line of sight; the equatorial velocity of rotation V_e; and the systemic velocity V_0. On the other hand, the second-degree Fourier representations of the observations summarized in Figs. (1), (2) and (3) give us directly a total of 42 Fourier coefficients. Through Eqs. (11), (12) and (13), it therefore becomes possible, at least in principle, to solve uniquely for the 35 Laplace coefficients and the additional unknown parameters χ, V_e, and V_0.

A first approximation to this solution has been carried out for HD 125248, with the results that are given in Table 1. As a check upon the solution, we must require that the radius of the star, as computed in the relation $R = PV_e/2\pi$, be appropriate for a main-sequence star near spectral type A 0. In addition, if we suppose that the variations in local equivalent width are due primarily to abundance irregularities and not to transfer differences over the surface of the star, we must obtain distribution functions that are non-negative over the whole surface. The first of these conditions is well-satisfied by the solution in Table 1. The computed radius is $2{\cdot}5\,\odot$, which is normal for a B 9 dwarf. Moreover, the solution yields $V_e \sin\chi = 6{\cdot}9$ km/sec,

Table 1. *Adopted constants for* HD 125248

Epoch of zero phase, $\Phi = 0$. JD 2430143·07. Period, $P = 9{\cdot}2983$ days.
Systemic velocity, $V_0 = -14{\cdot}3$ km/sec. Stellar radius, $R = 2{\cdot}5\,R_\odot$.
Rotational velocity, $V_e = 13{\cdot}7$ km/sec. Inclination, $\chi = 30°$.
Limb coefficients: $\mu = 0{\cdot}62$ in the continuum; $\kappa = 0{\cdot}18$ in the lines.

Laplace coefficients

	a_0^0	a_1^0	a_1^1	α_1^1	a_2^0	a_2^1	α_2^1	a_2^2	α_2^2
A	2·50	−2·80	1·50	−0·90	1·36	−0·12	0·06	0·15	−0·24
B	2·75	−2·75	−0·30	0·28	0·06	−0·43	0·36	0·12	0·24
C	2·50	−2·50	0·60	−0·16	0·50	−0·05	0·09	0·12	−0·15
	m_0^0	m_1^0	m_1^1	μ_1^1	m_2^0	m_2^1	μ_2^1	m_2^2	μ_2^2
H (kilogauss)	0	5·20	2·80	−1·00	−0·50	0·40	0·00	−1·50	0·00

Fourier coefficients

	d_0	d_{-1}	δ_{-1}	d_{-2}	δ_{-2}	$\overline{W}/\langle W\rangle$	Elements
A	1	0·40	−0·25	0·04	−0·06	0·918	Eu II, Gd II, Ce II
B	1	−0·48	0·41	0·03	0·06	1·117	Cr I, Cr II, Sr II
C	1	0·16	0·03	0·03	−0·04	0·983	Fe I, Fe II, Ti II
	e_0	e_{-1}	ϵ_{-1}	e_{-2}	ϵ_2		
A	0	0·176	0·289	0·087	0·054		
B	0	−0·122	−0·139	−0·087	0·044		
C	0	0·017	0·115	0·054	0·044		
	g_0	$g_{-1}+g_1$	$\eta_{-1}-\eta_1$	$g_{-2}+g_2$	$\eta_{-2}-\eta_2$		
A	1·00	2·43	−1·05	−0·20	−0·14		
B	−0·61	1·57	−0·40	−0·38	0·04	(kilogauss)	
C	0·59	1·97	−0·62	−0·27	0·03		

which is consistent with the widths of the relatively non-variable lines in the spectrum of this object[5]. The condition that ξ must be non-negative is not satisfied; for groups A and B, the distribution functions do go slightly negative over certain small areas. It would seem, however, that relatively small changes in some of the Laplace coefficients could remedy these defects in the solution, without appreciably changing its character.

In Figs. 5, 6 and 7, the observations are compared with the solution of Table 1. Only the mean points for each group of elements have been plotted on these figures. In the case of Fig. 6, the observed quantities differ slightly from those in Fig. 2, because the average equivalent widths $\overline{W}$ at the *observed* phases have been replaced by the averages $\langle W \rangle$ over the whole cycle.

The geometry of the resulting configuration is illustrated by the maps in Figs. 8, 9 and 10. The first two figures give the contours of the distribution functions, on an Aitoff equal-area projection. Fig. 9 also gives the contours of $|\mathbf{H}|$, the magnitude of the local magnetic field. The solution has the property that it will satisfy the observations equally well if the contours are reflected in the equator, together with the path of the subsolar point. Fig. 10 gives an orthographic projection in the plane of the sky. It illustrates the aspect changes with phase.

The probable errors of the observations in Figs. 5, 6 and 7 are such that many of the residuals from the computed curves are undoubtedly significant. These residuals could presumably be somewhat improved by a least squares adjustment of the Laplace coefficients to the observations. The method of solution that has been actually used is a crude one, and is not entirely systematic. On the other hand, some of the discrepancies between the computed curves and the observations may be attributable to the effects of the higher-order terms that have been neglected. In particular, the second-order Laplace coefficients are sufficiently large in some cases as to indicate that, in a systematic scheme of approximation, it would be necessary to consider certain higher-order terms that have been neglected in this treatment.

The solution that has been obtained here is further impaired by the neglect of the brightness variation that is known to occur over the surface of the star[6]. The amplitude of the observed light curve is only 0·05 magnitude, but this could imply relatively large local variations of brightness. If these are accompanied by temperature changes in the reversing layer, the assumption that all lines can be represented by a single linear curve of growth might also require modification.

Even without these complications, the solution must still be investigated with respect to its stability. In these circumstances, it seems reasonable to

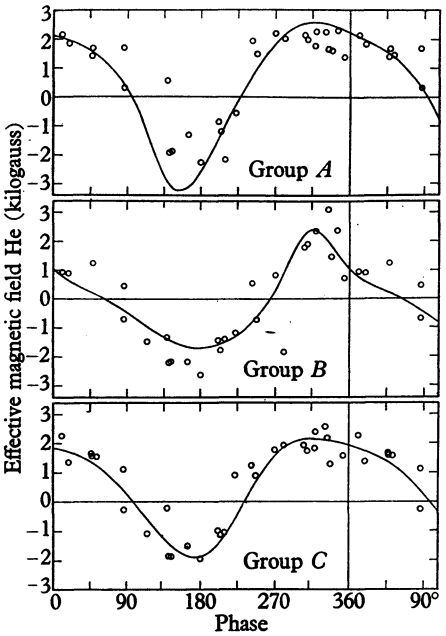

Fig. 5

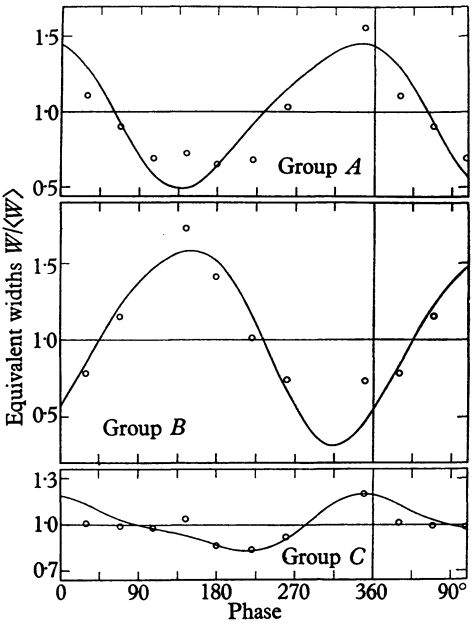

Fig. 6

Fig. 5. Effective magnetic field, H_e, in kilogauss. From the measures of H. W. Babcock[2]. The smooth curves have been computed from the constants of Table 1.

Fig. 6. Equivalent widths of 127 absorption lines. The mean points are the same as in Fig. 2, except that a small correction has been applied to change $\overline{W}$ to $\langle W \rangle$, the equivalent width averaged over the whole cycle. The smooth curves have been computed from the constants of Table 1.

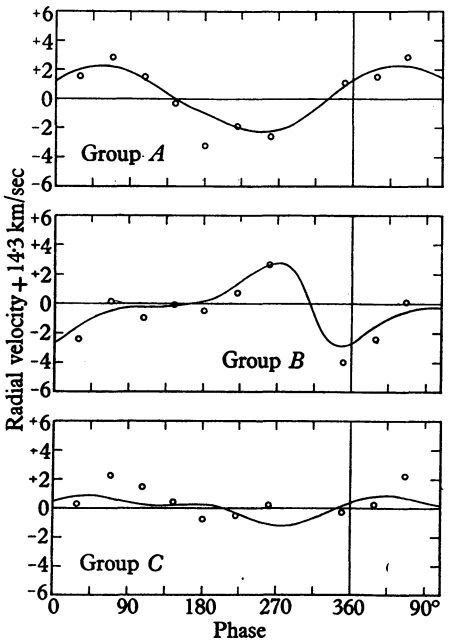

Fig. 7. Radial velocities from 127 absorption lines. The smooth curves have been computed from the constants of Table 1.

https://doi.org/10.1017/S0074180900237807 Published online by Cambridge University Press

suppose that only the principal large-scale features of the solution can be considered as established. More detailed discussions, based on more extensive observations, may be indicated for the future.

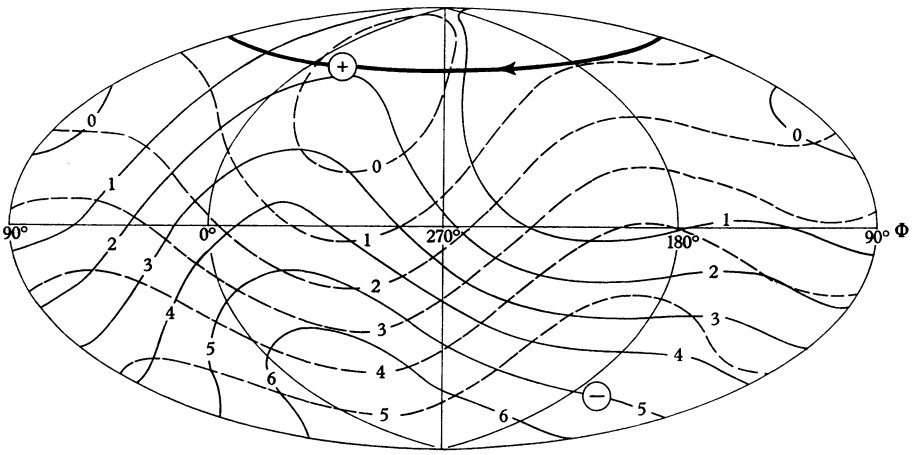

Fig. 8. Curves of constant local equivalent width for the lines of Group *A* (Eu II, Gd II, and Ce II; full curves) and Group *B* (Cr I, Cr II, and Sr II; broken curves). The subsolar point describes the heavy curve in the direction indicated; it lies at longitude $v=0$ at phase $\Phi=0$. The plus and minus signs mark the axis of the magnetic dipole. Aitoff equal-area projection.

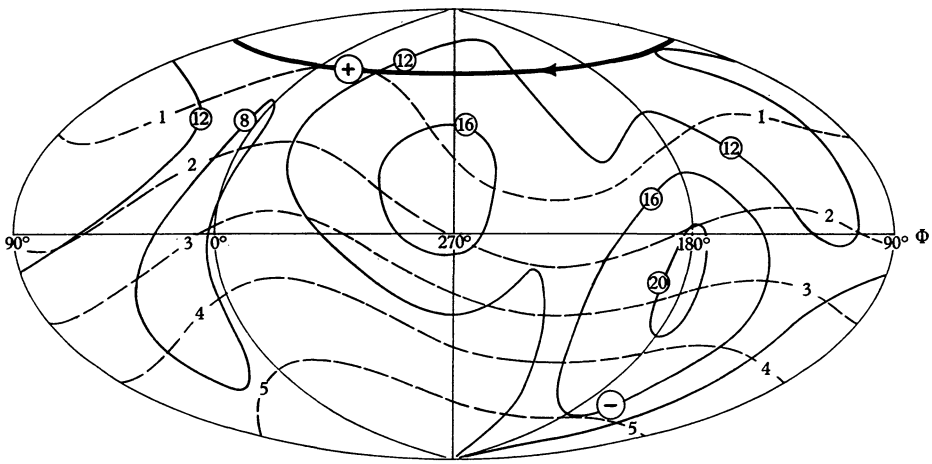

Fig. 9. The dashed curves are curves of constant local equivalent width for the lines of Group *C* (Fe I, Fe II, Ti II). The full curves are the contours of $|\mathbf{H}|$. The heavy curve and the plus and minus signs have the same significance as in Fig. 8.

An interesting feature of the solution is the situation of all three abundance maxima in the unobserved zone of the star. A calculation has shown that if this configuration were observed under an inclination of $\chi=150°$,

instead of 30°, all three groups of lines would be about four times stronger when averaged over the cycle. The amplitudes of the curves giving H_e and V as a function of phase would be comparable with the values actually observed. But the amplitudes of the curves for $W/\langle W\rangle$ would be less than

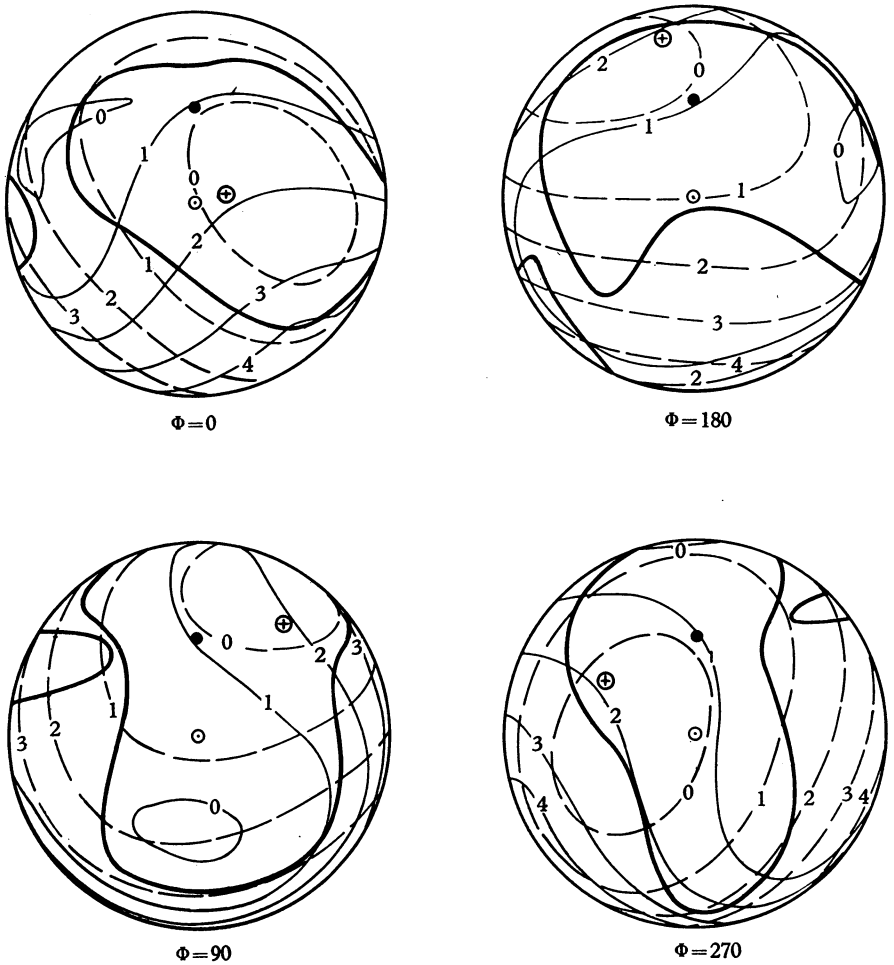

Fig. 10. Orthographic projections of the visible hemisphere on the plane of the sky at four phases. The light curves are the contours of Fig. 8. The poles of the dipole are indicated. The heavy curve is the locus where $H_z=0$.

one-third as great, because of the increase in $\langle W\rangle$. It is possible that aspect effects of this kind could account for some of the magnetic variable stars that do not show conspicuous spectrum variation.

There is some evidence for secular changes in this star, in addition to the short-period effects that have been attributed here to mere aspect

changes associated with rigid rotation. In all probability, these additional changes represent actual distortions of the configuration derived above. If so, they will have to be discussed within the theoretical framework of hydromagnetics. Such changes may also give rise to the acceleration phenomena that are required if nuclear processes occur in the atmosphere, as envisaged by Fowler and the Burbidges [7]. Meanwhile, we require a physical interpretation of the large-scale semi-rigid configuration derived above.

REFERENCES

[1] Babcock, H. W. This symposium, Paper 19.
[2] Babcock, H. W. *Astrophys. J.* **114**, 1, 1951.
[3] Deutsch, A. J. *Publ. A.S.P.* **68**, 92, 1956.
[4] Satô, Y. *Bull. Earthquake Research Inst., Tokyo*, **28**, 175, 1950.
[5] Deutsch, A. J. *I.A.U. Transactions*, vol. 8 (Rome, 1952), Cambridge University Press, 1955, p. 801.
[6] Stibbs, D. W. N. *Mon. Not. R. Astr. Soc.* **110**, 395, 1950.
[7] Burbidge, G. R. This volume, p. 222.

Discussion

Schatzman: I apologize for suggesting a slight increase in complications to the scheme of Dr Deutsch. It seems necessary to take into account the process of line formation in the expression of the weight functions used in numerator and denominator. In the more simple case of pulsating variable stars, Mlle Duquesne and myself have found that the ratio of the observed radial velocity to the material radial velocity is not 17/24 as usually assumed but is smaller by about 30 %.

Deutsch: I was aware that I have used a very approximate relation for the limb-weakening of lines, but in this context it seems adequate. It is surprising to find out how large the effect is for a scattering atmosphere on a Milne–Eddington model. It comes out that for an A-type star you can expect moderately strong lines to be something like 20 % weaker at the limb than they are at the centre of the disk.